

~~CONFIDENTIAL~~

7
Copy
RM E56C09

NACA RM E56C09

6.2

NACA

RESEARCH MEMORANDUM

ATTENUATION OF TANGENTIAL-PRESSURE OSCILLATIONS IN A
LIQUID-OXYGEN - n-HEPTANE ROCKET ENGINE WITH
LONGITUDINAL FINS

By Richard J. Priem

Lewis Flight Propulsion Laboratory
Cleveland, Ohio

CLASSIFICATION CHANGED

to UNCLASSIFIED

By authority of NASA memo Dated Mar. 12, 1963

s/ P. M. Lovell for

Boyd C. Myers II

CLASSIFIED DOCUMENT

This material contains information affecting the National Defense of the United States within the meaning of the espionage laws, Title 18, U.S.C., Secs. 793 and 794, the transmission or revelation of which in any manner to an unauthorized person is prohibited by law.

NATIONAL ADVISORY COMMITTEE
FOR AERONAUTICS

HR-6-25-63

WASHINGTON

June 28, 1958

~~CONFIDENTIAL~~

NATIONAL ADVISORY COMMITTEE FOR AERONAUTICS

RESEARCH MEMORANDUM

ATTENUATION OF TANGENTIAL-PRESSURE OSCILLATIONS IN A LIQUID-

OXYGEN - n-HEPTANE ROCKET ENGINE WITH LONGITUDINAL FINS

By Richard J. Priem

SUMMARY

In an effort to prevent high-frequency combustion-pressure oscillations (screaming), fins were installed in the combustion chamber of a 1000-pound-thrust rocket engine with a chamber pressure of 300 pounds per square inch and using liquid oxygen and n-heptane as propellants.

Tangential combustion-pressure oscillations were eliminated with longitudinal fins located in the combustion zone. The fin position for the liquid-oxygen - n-heptane engine was different from that of the nitric acid - JP-4 fuel system investigated by Theodore Male and William R. Kerslake. With four fins 4 inches or more in length, complete elimination of the traveling form of the tangential-pressure oscillation was obtained when the fronts of the fins were 3 inches or less from the injector face.

With the fronts of the fins located 4 or more inches from the injector face, tangential oscillations were not eliminated; however, the frequency of their occurrence was reduced about 40 percent.

The amplitudes of the pressure oscillations were estimated from streak photographs. Fins were relatively ineffective in reducing the amplitude of the pressure oscillations (measured between the injector and fins) in runs where oscillations occurred with fins. Amplitude decreased with increasing chamber length.

Unsymmetrical injection patterns were briefly investigated. These injectors had about the same probability of screaming as those with symmetrical injection patterns and the same amplitude of the pressure wave.

All tests were 0.75 second long.

INTRODUCTION

The occurrence of high-frequency combustion-pressure oscillations (screaming) associated with a resonant frequency of the combustion chamber

is a major problem in the development of rocket engines. These oscillations cause increased heat-transfer rates, which result in engine burnouts. Oscillations in particular engines have been eliminated by changes in injector design, nozzle configuration, and starting sequence, but these methods are not always effective in other engines.

Several basic techniques for attenuating and eliminating oscillations have been investigated experimentally. Longitudinal fins prevented screaming in a 1000-pound-thrust, nitric acid - JP-4 fuel rocket engine (ref. 1). Acoustical absorbers and changes in injector configuration have been used for attenuation of longitudinal oscillations in several rocket engines (refs. 2 and 3). Perforated liners have prevented lateral oscillations in turbojet afterburners (ref. 4).

The work of reference 1 was extended to determine whether fins would eliminate screaming in a 1000-pound-thrust rocket engine using liquid oxygen and n-heptane as a propellant combination. This report considers the effect of fin position, fin length, oxidant-fuel weight ratio, and chamber length on the screaming probability of a liquid-oxygen - n-heptane engine. To determine whether changes in injector distribution could eliminate screaming, injectors producing unsymmetrical mass flow and distributions of oxidant-fuel weight ratio were also used.

The occurrence and strength of the oscillations were determined by photographing the combustion gases through a narrow window with a continuous-moving-strip camera. The window was perpendicular to the longitudinal axis of the chamber.

EQUIPMENT

Engine. - The rocket engine was designed for a thrust of 1000 pounds and a chamber pressure of 300 pounds per square inch. A 4-inch-diameter cylindrical combustion chamber and a convergent-divergent nozzle were used (fig. 1).

The combustion chamber had interchangeable sections so that the chamber length could be varied from 2 to 29 inches. The engine was also equipped with a 1/4-inch transparent Lucite ring for viewing the combustion gases. This ring was always located $1\frac{1}{2}$ inches from the face of the injector. Figure 2 shows a disconnected assembly of the engine parts. A spark plug was used for starting.

Uncooled fins made of steel bar stock (1 by 1/2 in.) were located in the chamber at distances of 2 to 18 inches from the face of the injector. Four fins were always used for these tests, and the length of the fins varied between 4 and 26 inches.

Injectors. - Schematic drawings of the five different injectors used in this investigation are shown in figure 3. Injector A (basic), which was used for most of the investigation, was an annular triplet design with two oxidant streams impinging on one fuel stream. The same injector design was used in references 1 and 5 and is described therein.

The remaining four injectors were designed to produce uneven propellant distribution in the chamber. Injector B had all 24 sets of impinging jets in an arc encompassing seven-eighths of a circle. Injector C had the injector divided into four quadrants. In the second and fourth quadrants the injector was identical to the basic injector. In the first and third quadrants the distance between the center of the injector and fuel orifices was reduced from 1.375 to 0.687 inches.

Injector D had alternate sets of large and small injector holes. Injector E had the propellant jets turned an additional 20° towards the chamber axis in the second and fourth quadrants.

Propellants. - In all cases the oxidant was liquid oxygen and the fuel was n-heptane.

Instrumentation. - Rocket-engine thrust was measured by a strain-gage load cell (accuracy, ± 2 percent). Propellant flows were measured by rotating-vane-type flowmeters (accuracy, ± 3 percent). Average chamber pressure was measured by a recording Bourdon-tube gage (accuracy, ± 3 percent).

A continuous-moving-film 16-millimeter camera was used for detecting and measuring screaming phenomena. The film speed varied between 60 and 110 feet per second. To obtain lateral streak records, the camera was so oriented that the film would move perpendicular to the window slit; consequently, the film moved parallel to the gas flow. Figure 4 is a schematic illustration of the method of lateral streak photography.

OPERATIONAL PROCEDURE

The rocket was operated by the following procedure: Automatic recording instruments were turned on, and the liquid-oxygen propellant valve was opened 0.85 second later and began closing at 1.65 seconds. The fuel propellant valve was opened at 1.00 second and began closing at 1.60 seconds. The camera was started at 1.00 second. The spark plug was energized for the entire run. This procedure gave a total running time of 0.75 second.

ANALYSIS OF PHOTOGRAPHIC DATA

Four different types of combustion were observed in this study. In addition to smooth combustion, three forms of oscillatory combustion

occurred: the longitudinal mode, and the standing and traveling forms of the tangential mode. The velocity and pressure distributions of the tangential modes are shown schematically in figure 5. The nomenclature in this report is the same as used in reference 6. The standing form of the tangential mode of oscillation consists of a pressure wave that travels diametrically from one side of the chamber to the other. The traveling wave form of the tangential mode of oscillation has a pressure wave that travels circumferentially around the chamber. The longitudinal mode is characterized by a pressure wave that travels between the injector and the nozzle.

Each of the four types of combustion produces different images on the moving film (fig. 6). Smooth combustion (fig. 6(a)) has random streaks with no distinct periodic motion or patterns. For the longitudinal oscillations (fig. 6(b)), a bright band appears on the film each time the wave crosses the window. This photograph was taken close to the injector; therefore, the wave traveling towards the injector is almost superimposed on the wave traveling from the injector.

The tangential modes of oscillation produce different photographs depending on the wave form and the orientation of the camera with respect to the wave (figs. 6(c), (d), and (e)). With the traveling wave form there is a bright band running diagonally across the film (fig. 6(c)). Superimposed on this band is a wave pattern of the combustion streaks. With the standing wave two different pictures are obtained, depending on the orientations of the camera to the wave. When the camera views the node point (position of maximum pressure variation and zero displacement), a bright band appears on the film and the combustion streaks are relatively straight (fig. 6(e)). When the camera views the anti-node point (position of zero pressure variation and maximum displacement), the standing wave produces the photograph shown in figure 6(d). There are no bright bands, but the combustion streaks have a wave pattern.

The various forms of the tangential oscillations can be determined more readily by viewing the chamber simultaneously from two different angles as illustrated in figures 6(f) and (g). The traveling wave produces almost identical photographs in both views as seen in figure 6(f). The standing wave produces the two images described previously if the camera is aligned with the nodes as shown in figure 6(g).

RESULTS

Engine Performance with Injector A

The performance of the engine was determined from the specific impulse

$$I = \frac{F}{W}$$

(All symbols are defined in appendix A.) Figure 7 shows the variation of specific impulse with the oxidant-fuel weight ratio o/f . Most of the data fall between 90 and 100 percent of theoretical specific impulse. The performance obtained with various chamber lengths is shown in figure 8. The performance at first increases with chamber length, but there is little change above 8 inches. The experimental scatter is approximately ± 5 percent.

3987 The change in performance with screaming is illustrated by the histogram of figure 9. The percentages were obtained by dividing the number of runs within 2-percent performance intervals by the total runs. This plot shows that with smooth combustion the peak of the histogram is at a performance of 93 percent of theoretical specific impulse. With screaming combustion the peak is shifted to 95 percent of theoretical specific impulse. Apparently a small increase in performance accompanies screaming. A summary of the performance data is given in table I.

Effect of Fins with Injector A

Oxidant-fuel weight ratio less than 2.5. - In the range of o/f from 1.5 to 2.5, 61 percent of the runs without fins had the traveling wave form of oscillation (table I). The other 39 percent of the runs were smooth. If fins were placed in the chamber so that the fronts of the fins were 3 inches or less from the injector face, all the runs were smooth (fig. 10). If the fronts of the fins were placed 4 inches or more from the injector face, 39 percent of the runs had the traveling wave form and 61 percent were smooth. Fin position and length are shown schematically in figure 10(a) with the type of combustion encountered.

Oxidant-fuel weight ratio greater than 2.5. - In the range of o/f from 2.5 to 4.0, 97 percent of the runs without fins had the traveling wave form. The other 3 percent of the runs were smooth. If fins were placed in the chamber so that the fronts were 3 inches or less from the injector face, 10 percent of the runs had the standing wave form and 90 percent were smooth runs. If the fronts of the fins were placed 4 inches or more from the injector face, 45 percent of the runs had the traveling wave and 29 percent had the standing wave. The standing wave usually occurred with chamber lengths between 14 to 21 inches as shown in figure 10(b).

Strength of waves. - The strength of the traveling wave form of the tangential oscillation at a distance of $1\frac{1}{2}$ inches from the injector face was estimated by the technique described in appendix B. Figure 11 illustrates the variation of pressure amplitude with length. The amplitude at first decreased with increasing length, but there is little change in amplitude for lengths greater than 11 inches. The observed variations in

wave pressure are shown by the histogram of figure 12. Without fins in the chamber the histogram peaked at a ratio of wave pressure to chamber pressure of 0.32. With fins in the chamber the peak of the histogram was decreased slightly to a ratio of 0.29.

Effect of Injector Design on Screaming Probabilities

The ratio of screaming runs to total runs for the various injectors is given in the following table:

Injector	Oxidant-fuel weight ratio, 1.5 to 2.5		Oxidant-fuel weight ratio, 2.5 to 4.0	
	<u>Screaming runs</u> Total runs	Screaming runs, percent	<u>Screaming runs</u> Total runs	Screaming runs, percent
A	15/25	60	26/27	96
B	1/3	33	3/5	60
C	0/1	0	3/3	100
D	1/1	100	1/1	100
E	0/1	0	2/2	100

All the injectors produced some screaming runs. The only injector which indicated a decrease in the screaming probability was injector B (fig. 3) which decreased the probability about 30 percent. This deduction is made on the basis of two to four runs and, therefore, does not represent the true probability. All injectors had about the same range of amplitude (fig. 11).

Destructiveness of Screaming

The destruction of the engine when operating under screaming conditions was evaluated by observing the erosion and burning of various engine components. The greatest burning occurred in the spark plug. This increased burning could result from an increase in the heat-transfer coefficient or from a peculiarity of the spark plug. Very little burning took place with smooth runs or runs with longitudinal pressure oscillations (fig. 13(a)). Only the outer electrode was eroded with these two types of combustion.

With the standing wave, the burning of the spark plug differed with its various locations. When the spark plug was located at the node point (position of maximum pressure variation), the center electrode and

porcelain were eroded when oscillations occurred (fig. 13(c)). At the anti-node point (position of zero pressure variation), only part of the porcelain was removed (fig. 13(d)).

The burning of the injector face illustrated in figure 14 shows the burning that occurred with 60 runs of 0.75-second duration each. The burning was inside the injector-orifice ring in contrast to the burning observed with nitric acid in reference 1, where it was outside the ring.

The amount of burning of the fins is shown in figure 15. Four unused fins and four fins used in the chamber for two runs of 0.75 second are shown. Most of the burning was on the upstream edge of the fins.

DISCUSSION

The critical location of the fins required to eliminate combustion-pressure oscillations are also observed in reference 1 which finds that, with a similar engine using nitric acid and JP-4 as propellants, the critical fin location is 8 to 16 inches from the injector. It is speculated that this location is a function of the regions of high heat release. With the liquid-oxygen - n-heptane system reported herein, maximum attenuation was obtained when fins were located in the region 2 to 8 inches from the injector face as shown in figure 10. This region also corresponds to the high energy release or combustion zone as shown in figure 8. Therefore, it can be concluded that maximum attenuation is obtained when the fins are in the combustion zone. Thus optimum fin location is a function of the injector and propellants.

Fins located beyond the combustion zone produced little effect on the amplitude of the wave moving in the combustion zone (fig. 12) and were relatively ineffective in eliminating screaming as shown in figure 10. In order to be effective, fins must therefore remove energy from the pressure wave at the location where the wave is receiving energy. Fins outside the combustion zone absorb some energy, but not necessarily enough to prevent oscillations.

The investigation of the effect of unsymmetrical distribution of mass flow and o/f on screaming occurrence has shown that the occurrences of screaming can be reduced by varying the injector design. However, unsymmetrical injector designs do not appear to be a technique for preventing screaming. Such schemes could be incorporated with other techniques, which in themselves could not eliminate screaming, thereby combining the effects to prevent destructive oscillations.

SUMMARY OF RESULTS

The investigation of attenuation of tangential combustion-pressure oscillations with longitudinal fins reported in an investigation by Theodore Male and William R. Kerslake was extended to a 1000-pound-thrust rocket engine with a chamber pressure of 300 pounds per square inch and using liquid oxygen and n-heptane as propellants. The combustion chamber was 4 inches in diameter and had a variable length of 2 to 29 inches. All tests were 0.75 second long. Four fins were attached axially to the chamber wall in symmetrical positions equidistant from the injector.

The results of this investigation are:

1. Tangential oscillations were prevented with fins located within 3 inches of the injector.
2. Occurrence of tangential oscillations was reduced by 40 percent with fins located 4 inches or more from the injector.
3. Fins that did not eliminate oscillations also did not appreciably reduce the amplitude of the oscillations observed $1\frac{1}{2}$ inches from the injector.
4. Performance values accompanying screaming were distributed about a mean of 95 percent of theoretical specific impulse; for smooth combustion, about a mean of 93 percent.
5. Tangential pressure oscillations produced more engine damage than longitudinal oscillations or smooth combustion.
6. Injectors that produced unsymmetrical distributions of mass flow and oxidant-fuel weight ratio did not eliminate oscillations.

Lewis Flight Propulsion Laboratory
National Advisory Committee for Aeronautics
Cleveland, Ohio, March 13, 1956

APPENDIX A

SYMBOLS

a	speed of sound, in./sec
F	thrust, lb
I	specific impulse, lb-sec/lb
o/f	oxidant-fuel weight ratio
P	pressure, lb/sq in.
P _c	average chamber pressure, lb/sq in.
R	gas constant sq in./(sec ²)(°R)
s	film speed, in./sec
T	average gas temperature, °R
V	gas velocity with respect to stationary point, in./sec
v	gas velocity with respect to wave, in./sec
w	total propellant flow, lb/sec
X	camera magnification, length on film/length in engine
ρ	density, lb/cu in.

Subscripts:

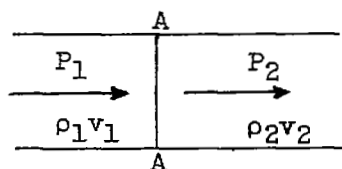
av	average
1	condition before shock
2	condition after shock

APPENDIX B

THEORY FOR CORRELATING WAVE PRESSURES WITH PARTICLE VELOCITIES

Some means of measuring the amplitude of the pressure wave is desirable in order to determine the effect of the fins on the intensity of the oscillations. This was obtained by correlating the wave pressure with the wave motion of the combustion streaks. However, this is a crude approximation because of the assumptions that one-dimensional-flow theory is valid, that the energy added to or lost in the wave can be neglected, that the ideal gas law represents the state of the gases, and that the shock wave moves at the speed of sound.

With these limitations in mind, the relation between particle velocity and wave pressure is obtained with the help of the following figure:



Gas is flowing toward a standing wave A-A at a velocity v_1 , pressure P_1 , and density ρ_1 . After the shock, the pressure is P_2 , velocity is v_2 , and density ρ_2 .

The momentum equations relate the increase in momentum of the gas per unit time to the net force acting on the gas in the same direction. For this case the equation becomes

$$P_1 + \rho_1 v_1^2 = P_2 + \rho_2 v_2^2 \quad (B1)$$

The continuity equation requires that

$$\rho_1 v_1 = \rho_2 v_2 \quad (B2)$$

Combining equations (B1) and (B2) gives the following equation:

$$v_2^2 - v_1^2 = (P_1 - P_2) \left(\frac{1}{\rho_2} + \frac{1}{\rho_1} \right)$$

The pressure rise across the wave is

$$P_2 - P_1 = (v_1^2 - v_2^2) \left(\frac{1}{\frac{1}{\rho_2} + \frac{1}{\rho_1}} \right)$$

If an average density ρ_{av} is used so that

$$\frac{2}{\rho_{av}} = \frac{1}{\rho_2} + \frac{1}{\rho_1}$$

and, if

$$\rho_{av} = \frac{P_c}{RT}$$

then

$$\frac{P_2 - P_1}{P_c} = \frac{v_1^2 - v_2^2}{2RT}$$

where $\frac{P_2 - P_1}{P_c}$ is defined as the wave strength.

If the wave is traveling at the speed of sound a , the velocities v_1 and v_2 are related to the velocities with respect to a stationary point s by

$$v_1 + a = V_1$$

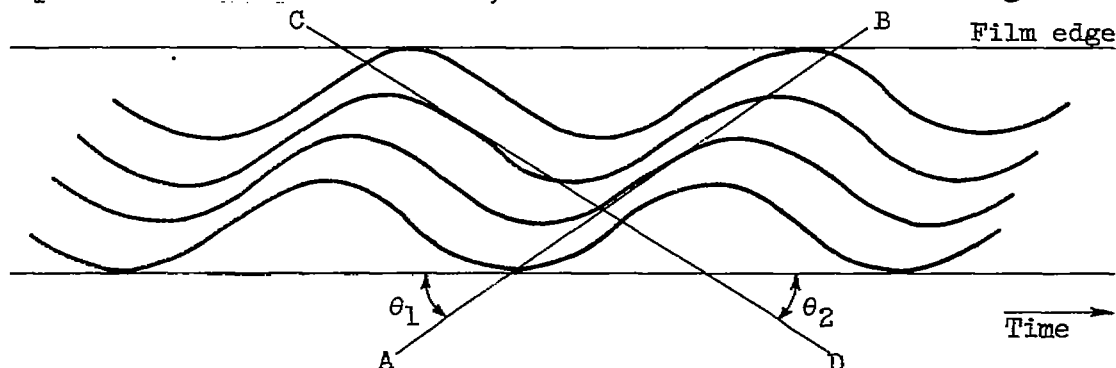
$$v_2 + a = V_2$$

Then

$$\frac{P_2 - P_1}{P_c} = \frac{(V_2 - V_1)a}{RT} + \frac{v_1^2 - v_2^2}{2RT}$$

The wave pressure is therefore determined by measuring the particle velocities before and after the wave has passed through the gas.

The particle velocities were determined from the film by the following technique. Tangents AB and CD were drawn to the maximum slope of the combustion streaks, as illustrated in the following sketch:



Particle velocities were then obtained from the following equation:

$$V_1 = \frac{s \tan \theta_1}{X}$$

REFERENCES

1. Male, Theodore, and Kerslake, William R.: A Method for Prevention of Screaming in Rocket Engines. NACA RM E54F28a, 1954.
2. Lawhead, Robert B., and Grossklaus, Albert A.: Rocket Engine Vibration Studies. Rep. AL-1590, Supplemental Summary Rep. for period ending Dec. 15, 1952, North American Aviation, Inc., Dec. 15, 1952. (Contract AF 33(038)-19430, Proj. MX 919.)
3. Anon.: Development of AJ11-9 Liquid-Propellant Booster Rocket. Rep. No. 611, Apr. 1, 1951-Mar. 31, 1952, Aerojet Eng. Corp., Nov. 20, 1952. (Boeing Subcontract, U.S. Air Force Contract AF 33(038)-19589, Proj. MX-1599.)
4. Lewis Laboratory Staff: A Summary of Preliminary Investigations into the Characteristics of Combustion Screech in Ducted Burners. NACA RM E54B02, 1954.
5. Male, Theodore, Kerslake, William R., and Tischler, Adelbert O.: Photographic Study of Rotary Screaming and Other Oscillations in a Rocket Engine. NACA RM E54A29, 1954.
6. Smith, R. P., and Sprenger, D. F.: Combustion Instability in Solid-Propellant Rockets. Fourth Symposium (International) on Combustion, The Williams & Wilkins Co., 1953, pp. 893-906.

TABLE I. - PERFORMANCE DATA OF 1000-POUND-THRUST ROCKET ENGINE

USING LIQUID OXYGEN AND n-HEPTANE AS PROPELLANTS

Run	Thrust, lb	Oxidant- fuel weight ratio	Total propellant flow rate, lb/sec	Specific impulse, lb-sec/lb	Chamber length, in.	Fins		Type of combustion oscillation
						Begin	End	
1	1030	3.35	4.61	223	19	None	None	^a Traveling
2	1070	4.50	5.01	213	19			Traveling
3	1040	3.25	4.25	244	19			Traveling
4	1100	4.16	4.96	230	19			Traveling
5	1090	3.64	4.64	235	19			Traveling
6	1120	2.65	4.61	243	19			Smooth
7	1130	2.31	4.73	239	19			Smooth
8	1100	3.95	4.79	229	19			Traveling
9	1060	1.82	4.62	230	19			Traveling
10	1080	3.89	4.68	233	19			Traveling
11	1108	4.08	4.77	235	34.5			Traveling
12	1130	2.06	4.60	245	34.5			Traveling
13	1030	2.35	4.45	254	34.5			Traveling
14	1110	3.10	4.56	248	34.5			Traveling
15	1130	3.72	4.82	235	34.5			Traveling
16	1110	4.17	4.78	232	14			Traveling
17	1140	3.00	4.59	248	14			Traveling
18	1150	2.05	4.65	247	14			Traveling
19	1080	3.75	4.75	225	20	6	10	Longitudinal
20	1085	2.11	4.71	231	20	6	10	Smooth
21	1110	3.77	4.77	232	20	None	None	Traveling
22	----	≈3.5	----	---	20	2	6	Longitudinal
23	----	≈2.0	----	---	20	2	6	Smooth
24	----	≈2.0	----	---	20	None	None	Traveling
25	1000	3.68	4.51	223	20	10	14	^b Standing
26	920	1.70	4.32	214	20	10	14	Traveling
27	850	1.74	4.01	212	20	10	14	Traveling
28	1180	3.60	4.67	262	20	8	12	Standing
29	945	1.78	4.50	215	20	8	12	Traveling
30	1100	3.55	4.69	235	20	None	None	Traveling
31	975	1.85	4.51	215	20	None	None	Traveling
32	1100	3.17	4.60	239	14	2	6	Standing
33	1085	2.76	4.52	239	14	2	6	Smooth
34	1160	2.43	4.58	252	14	2	6	Standing
35	1140	2.13	4.70	243	14	2	6	Smooth

^aTraveling wave form of tangential mode of oscillation.^bStanding wave form of tangential mode of oscillation.

TABLE I. - Continued. PERFORMANCE DATA OF 1000-POUND-THRUST ROCKET
ENGINE USING LIQUID OXYGEN AND n-HEPTANE AS PROPELLANTS

Run	Thrust, lb	Oxidant- fuel weight ratio	Total propellant flow rate, lb/sec	Specific impulse, lb-sec/lb	Chamber length, in.	Fins		Type of combustion oscillation
						Begin	End	
36	1105	3.55	4.81	229	14	4	8	Standing
37	1150	2.08	4.80	239	14	4	8	Smooth
38	1150	3.75	4.87	236	14	None	None	Traveling
39	1155	3.65	4.65	249	20	4	8	Standing
40	1100	3.67	4.77	230	14	6	10	Standing
41	998	1.80	4.33	229	14	6	10	Traveling
42	1170	2.03	4.97	235	14	6	10	Smooth
43	1075	3.13	4.42	242	23	6	10	Traveling
44	1090	2.07	4.67	233	23	6	10	Traveling
45	1105	3.65	4.77	231	23	None	None	Traveling
46	1115	2.02	4.38	253	23	None	None	Traveling
47	1105	3.35	4.67	237	23	4	8	Standing
48	1040	2.02	4.62	225	23	4	8	Smooth
49	1100	2.22	4.72	233	23	4	8	Smooth
50	1030	2.93	4.35	237	32	12	16	Traveling
51	1100	3.68	4.77	231	32	12	16	Traveling
52	1035	2.02	4.53	228	32	12	16	Traveling
53	1120	2.19	4.74	237	32	12	16	Traveling
54	1145	3.17	4.80	236	32	4	8	Smooth
55	1140	2.07	4.83	235	32	4	8	Traveling
56	1160	3.38	4.69	247	32	None	None	Traveling
57	1130	3.41	4.67	241	32	8	12	Traveling
58	1090	2.03	4.69	233	32	8	12	Traveling
59	1130	2.04	4.70	235	32	8	12	Traveling
60	1100	3.29	4.82	229	23	2	16	Smooth
61	----	^a 3.2	----	---	9	2	6	Smooth
62	----	^a 2.0	----	---	9	2	6	Smooth
63	----	^a 3.2	----	---	9	None	None	Traveling
64	----	^a 1.7	----	---	9	None	None	Traveling
65	1105	3.00	4.53	245	11.5	4.5	8.5	Smooth
66	1110	1.86	4.73	235	11.5	4.5	8.5	Standing
67	1165	3.45	5.03	232	11.5	4.5	8.5	Smooth
68	1105	3.00	4.67	237	16	5	9	Traveling
69	1190	2.16	4.99	239	16	5	9	Smooth
70	1170	3.45	4.77	245	16	5	9	Standing

TABLE I. - Continued. PERFORMANCE DATA OF 1000-POUND-THRUST ROCKET

ENGINE USING LIQUID OXYGEN AND n-HEPTANE AS PROPELLANTS

Run	Thrust, lb	Oxidant- fuel weight ratio	Total propellant flow rate, lb/sec	Specific impulse, lb-sec/lb	Chamber length, in.	Fins		Type of combustion oscillation
						Begin	End	
71	1210	2.06	5.11	237	16	None	None	Smooth
72	-----	≈3.5	-----	---	18	3	7	Standing
73	-----	≈2.0	-----	---	18	3	7	Smooth
74	-----	≈3.5	-----	---	18	None	None	Traveling
75	-----	≈2.0	-----	---	18	None	None	Smooth
76	1150	3.25	4.72	243	26	7	11	Traveling
77	1190	2.08	4.99	239	26	7	11	Smooth
78	1080	1.86	4.70	230	26	None	None	Traveling
79	-----	≈3.5	-----	---	25	9	13	Traveling
80	-----	≈2.0	-----	---	25	9	13	Smooth
81	-----	≈3.5	-----	---	25	None	None	Traveling
82	1170	3.21	4.63	253	25	4	8	Smooth
83	1180	2.07	4.99	234	25	4	8	Smooth
84	1050	1.72	4.73	222	25	None	None	Traveling
85	1190	3.52	5.00	237	25	13	17	Traveling
86	1200	2.21	5.15	231	25	13	17	Smooth
87	1170	2.19	5.02	231	25	13	17	Smooth
88	1160	3.26	4.95	233	23	6	10	Smooth
89	1180	2.10	5.02	233	23	6	10	Smooth
90	1170	2.22	5.15	227	23	6	10	Smooth
91	1180	3.53	5.07	233	23	6	10	Smooth
92	1150	2.98	4.74	243	23	3	7	Smooth
93	1160	1.96	4.92	237	23	3	7	Smooth
94	1250	2.53	5.09	244	23	3	7	Smooth
95	1130	3.36	5.06	223	23	3	7	Smooth
96	1160	3.50	4.82	241	23	12	16	Smooth
97	1140	1.91	4.95	231	23	12	16	Smooth
98	1190	2.08	5.18	230	23	12	16	Smooth
99	-----	≈2.94	-----	---	32	4	12	Smooth
100	-----	≈2.0	-----	---		4	12	Smooth
101	-----	2.10	-----	---	5	None	None	Traveling
102	-----	2.00	-----	---	5	None	None	Traveling
103	-----	2.84	-----	---	7	None	None	Traveling
104	-----	3.25	-----	---	7	None	None	Traveling
105	-----	2.86	-----	---	25	4	12	Smooth

TABLE I. - Continued. PERFORMANCE DATA OF 1000-POUND-THRUST ROCKET

ENGINE USING LIQUID OXYGEN AND n-HEPTANE AS PROPELLANTS

Run	Thrust, lb	Oxidant- fuel weight ratio	Total propellant flow rate, lb/sec	Specific impulse, lb-sec/lb	Chamber length, in.	Fins		Type of combustion oscillation
						Begin	End	
106	----	1.86	----	---	25	4	12	Smooth
107	----	2.00	----	---	25	None	None	Traveling
108	----	2.80	----	---	18	4	12	Traveling
109	----	1.93	----	---	18	4	12	Smooth
110	----	3.12	----	---		None	None	Traveling
111	----	2.85	----	---	17	10	14	Smooth
112	----	2.05	----	---	17	10	14	Smooth
113	----	1.97	----	---	17	None	None	Smooth
114	----	2.10	----	---	21	14	18	Traveling
115	----	2.04	----	---	21	14	18	Smooth
116	----	1.90	----	---	21	14	18	Traveling
117	----	3.70	----	---	21	14	18	Traveling
118	----	2.65	----	---	25	18	22	Traveling
119	----	2.05	----	---	25	18	22	Smooth
120	----	2.10	----	---	25	18	22	Smooth
121	----	3.70	----	---	19	10	14	Traveling
122	----	2.00	----	---	19	10	14	Smooth
123	----	2.00	----	---	20	7	9	Smooth
124	----	3.82	----	---	20	7	9	Traveling
125	----	2.75	----	---	20	7	9	Traveling
126	----	1.90	----	---	20	7	9	Smooth
127	----	3.60	----	---	20	7	9	Traveling
128	----	3.38	----	---	5	None	None	Traveling
129	----	1.95	----	---	5	None	None	Smooth
130	----	1.92	----	---	5	None	None	Smooth
131	----	2.90	----	---	13	None	None	Traveling
132	----	1.67	----	---	13	None	None	Traveling
133	----	1.61	----	---	13	None	None	Smooth
134	----	3.35	----	---	12	2	9	Smooth
135	----	1.85	----	---	12	2	9	Smooth

TABLE I. - Continued. PERFORMANCE DATA OF 1000-POUND-THRUST ROCKET
ENGINE USING LIQUID OXYGEN AND n-HEPTANE AS PROPELLANTS

Run	Thrust, lb	Oxidant- fuel weight ratio	Total propellant flow rate, lb/sec	Specific impulse, lb-sec/lb	Chamber length, in.	Fins		Type of combustion oscillation
						Begin	End	
136	----	3.60	----	---	12	None	None	Traveling
137	----	1.80	----	---	12	None	None	Traveling
138	----	3.40	----	---	32	2	29	Smooth
139	----	4.57	----	---	31	2	28	Smooth
140	----	2.18	----	---	31	2	28	Smooth
141	----	2.13	----	---	31	None	None	Smooth
142	----	4.52	----	---	31	None	None	Traveling
143	----	3.02	----	---	27	2	24	Smooth
144	----	1.98	----	---	27	2	24	Smooth
145	----	1.95	----	---	27	None	None	Smooth
146	----	2.93	----	---	27	None	None	Traveling
147	----	2.93	----	---	22	2	19	Smooth
148	----	3.08	----	---	22	2	19	Smooth
149	----	1.96	----	---	22	2	19	Smooth
150	----	2.01	----	---	22	None	None	Smooth
151	----	~3.0	----	---	17	2	14	Smooth
152	----	1.90	----	---	17	2	14	Smooth
153	----	1.78	----	---	17	None	None	Traveling
154	----	2.95	----	---	20	4	12	Standing
155	----	1.87	----	---	20	4	12	Smooth
156	----	3.20	----	---	20	4	12	Standing
157	----	2.55	----	---	20	4	10	Smooth
158	----	1.65	----	---	20	4	10	Traveling
159	----	~3.0	----	----	20	4	10	Standing
160	----	3.15	----	---	16	2	6	Smooth
161	1180	2.22	4.72	248	16	2	6	Smooth
162	1230	1.99	5.04	244	16	2	6	Smooth
163	1220	3.37	4.85	252	16	None	None	Traveling
164	1160	2.93	4.75	243	20	8	16	Traveling
165	1140	1.89	4.97	228	20	8	16	Smooth

TABLE I. - Concluded. PERFORMANCE DATA OF 1000-POUND-THRUST ROCKET
ENGINE USING LIQUID OXYGEN AND n-HEPTANE AS PROPELLANTS

Run	Thrust, lb	Oxidant- fuel weight ratio	Total propellant flow rate, lb/sec	Specific impulse, lb-sec/lb	Chamber length, in.	Fins		Type of combustion oscillation
						Begin	End	
166	1180	2.91	5.04	234	20	8	16	Smooth
167	1190	3.20	5.18	229	20	8	14	Smooth
168	1170	2.09	4.95	236	20	8	14	Smooth
169	1160	3.13	5.08	231	20	8	14	Standing
170	1160	3.00	5.14	228	20	8	14	Traveling
171	1180	3.15	5.08	231	20	8	12	Smooth
172	1150	1.95	4.91	235	20	8	12	Smooth
173	1180	2.98	5.14	230	20	8	12	Standing
174	1050	2.81	4.68	225	14	2	6	Smooth
175	1140	2.24	4.99	229	14	2	6	Smooth
176	1070	2.83	4.81	223	14	2	6	Smooth
177	870	1.54	4.36	200	14	None	None	Traveling
178	----	≈3.0	---	---	20	6	10	Smooth
179	1100	2.68	4.75	231	20	6	10	Traveling
180	1200	2.59	5.00	237	20	6	10	Standing
181	910	2.53	4.58	197	20	6	10	Standing
182	1100	2.34	4.88	225	20	6	10	Standing
183	1000	2.46	4.58	217	29	2	6	Smooth
184	1125	2.36	5.14	219	29	2	6	Smooth
185	1160	3.33	5.29	221	29	2	6	Smooth
186	1100	2.39	4.58	237	29	None	None	Traveling
187	1050	2.31	4.39	238	14	4	8	Standing
188	1030	1.70	4.67	223	14	4	8	Traveling
189	1130	3.32	4.84	233	14	4	8	Standing
190	1220	3.45	5.00	245	14	4	8	Standing
191	----	2.73	5.06	---	29	6	10	Traveling
192	----	2.13	5.15	---	29	6	10	Traveling
193	----	3.52	5.29	---	20	2	10	Smooth
194	----	3.02	4.94	---	20	2	10	Smooth
195	----	1.97	4.96	---	20	2	10	Smooth
196	----	≈3.27	5.12	---	20	2	10	Smooth
197	----	≈3.00	---	---	20	None	None	Traveling
198	----	3.11	5.02	---	29	12	16	Traveling
199	1080	1.83	4.78	227	29	12	16	Traveling
200	1150	3.50	4.72	243	29	None	None	Traveling
201	1240	2.85	4.81	252	9.5	None	None	Traveling

3757

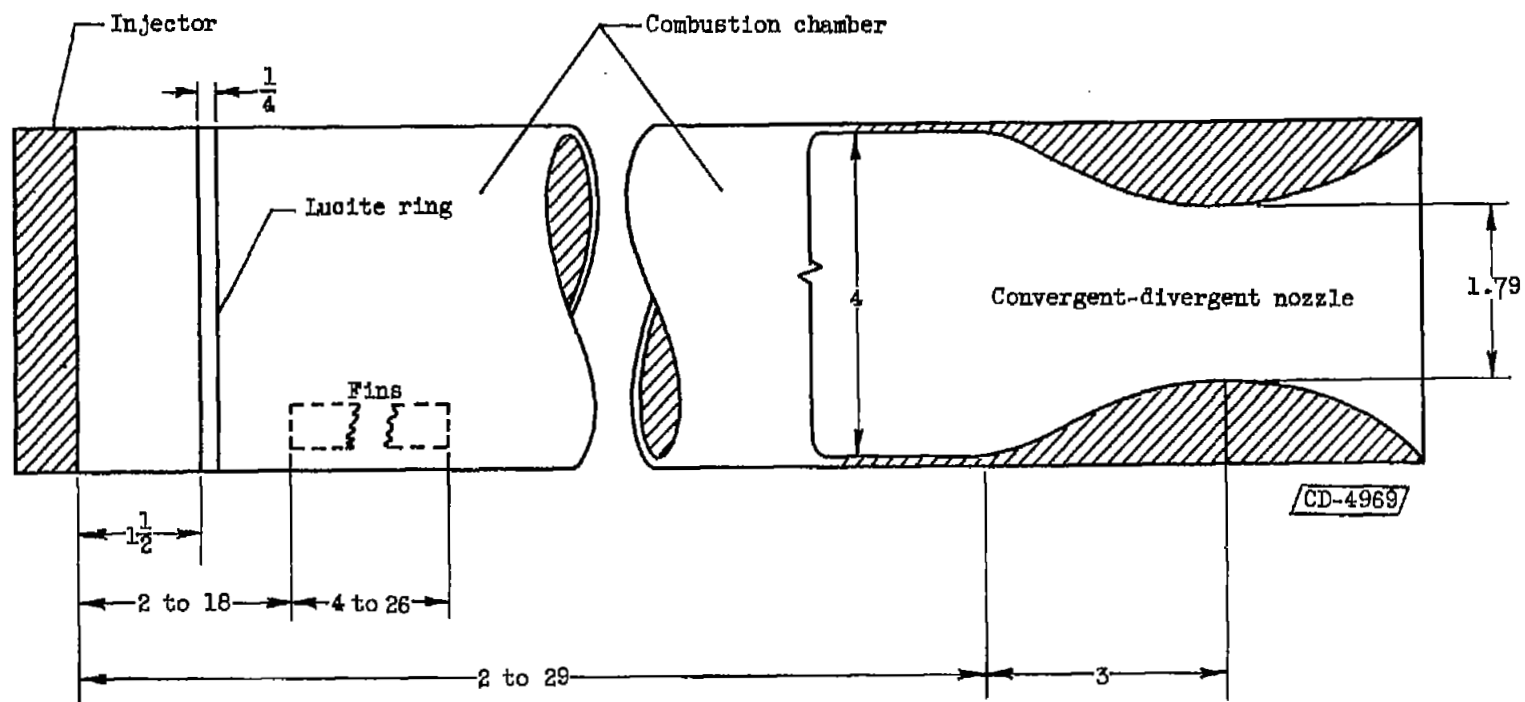
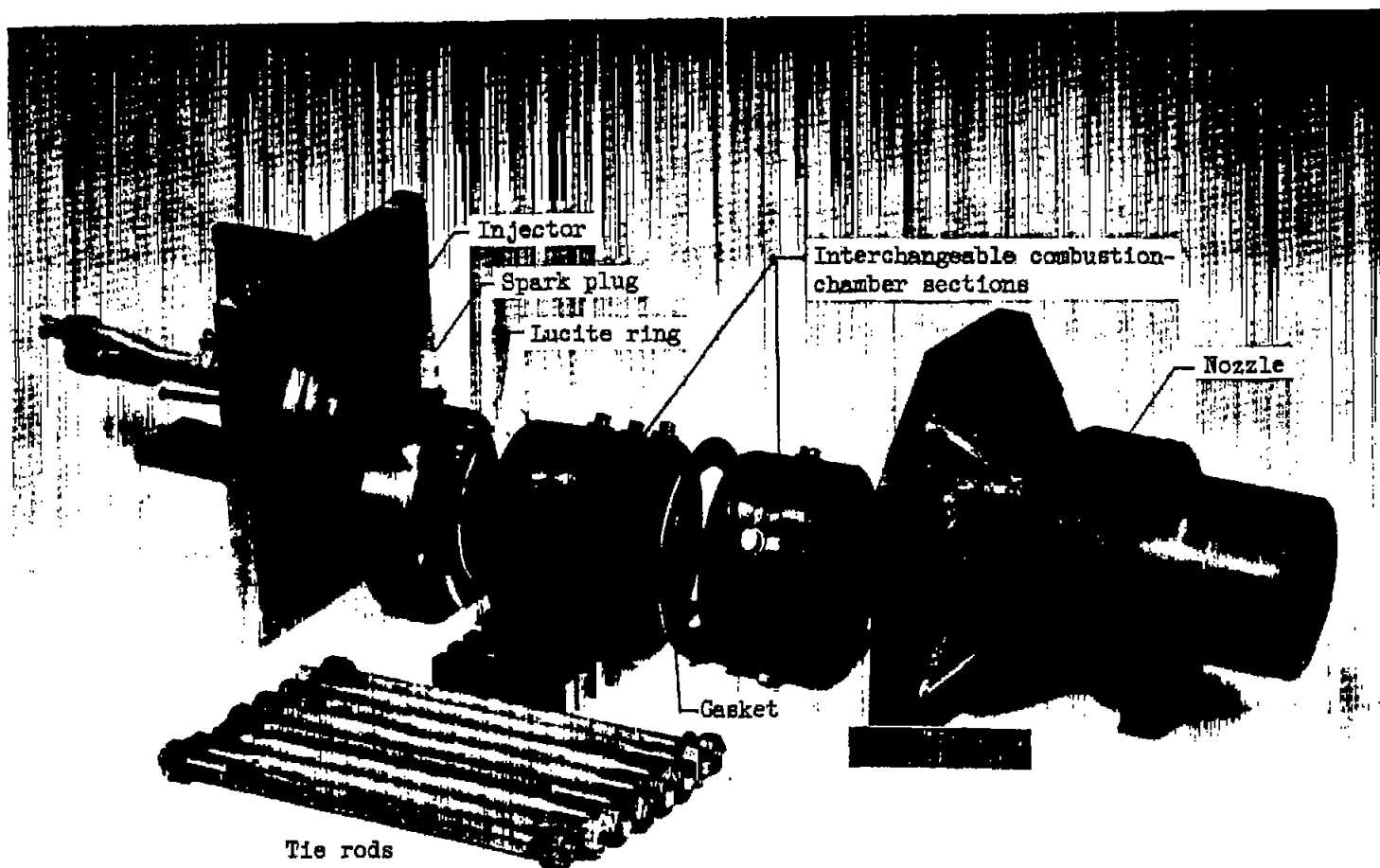
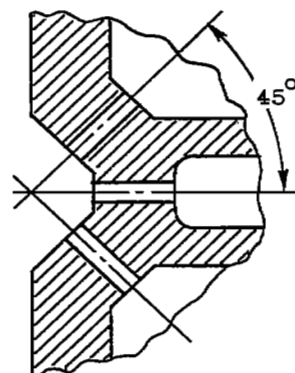
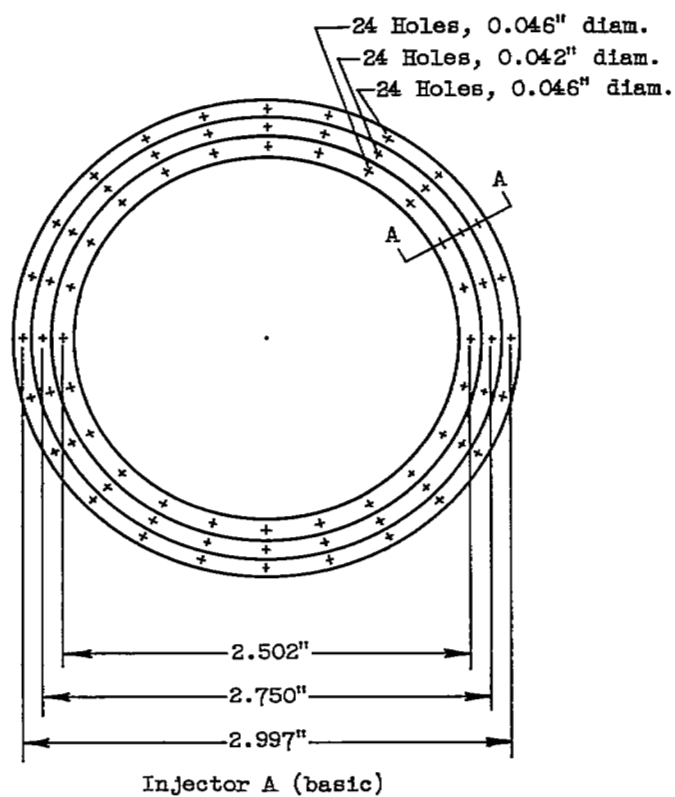


Figure 1. - Engine. (All dimensions in inches.)



C-40225

Figure 2. - Disconnected engine assembly.



Section A-A

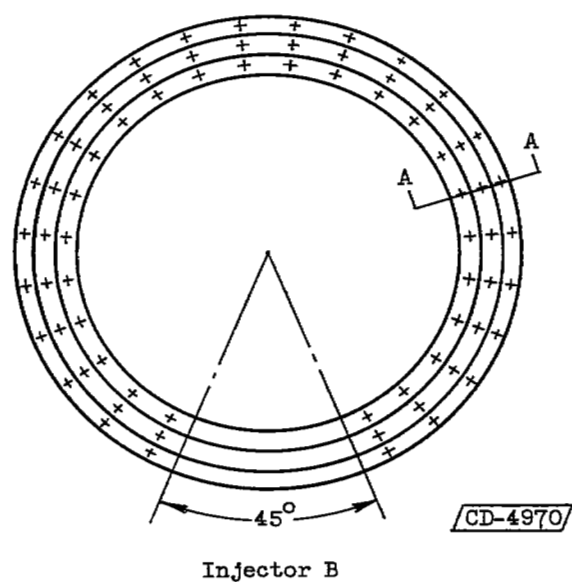
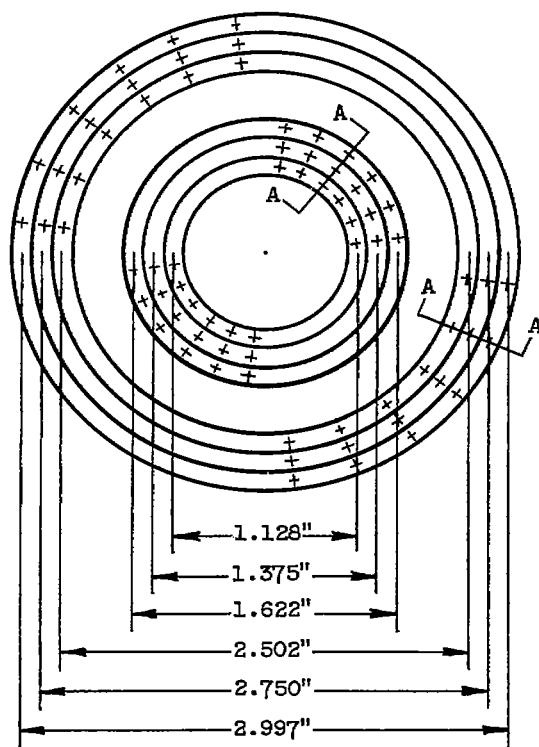
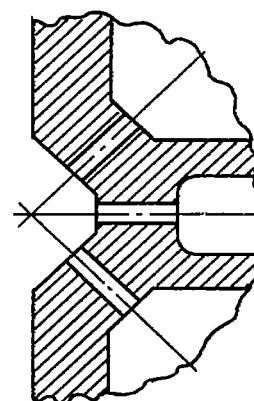


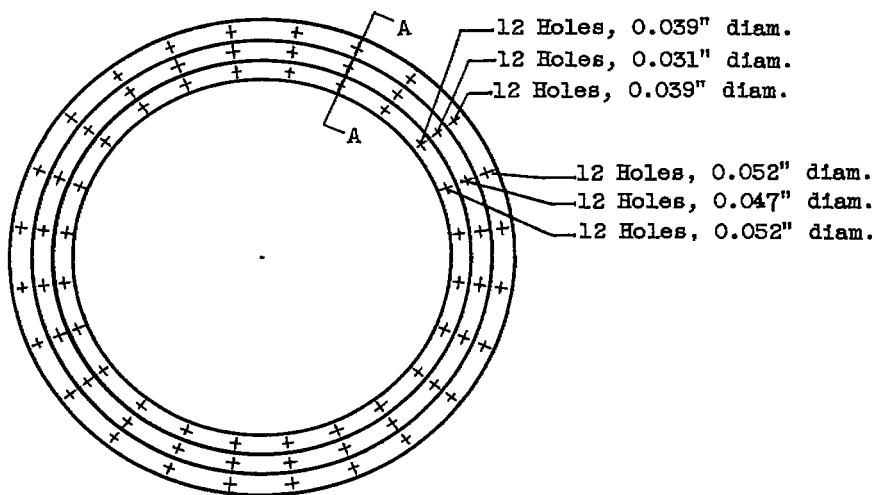
Figure 3.3 Injectors.



Injector C



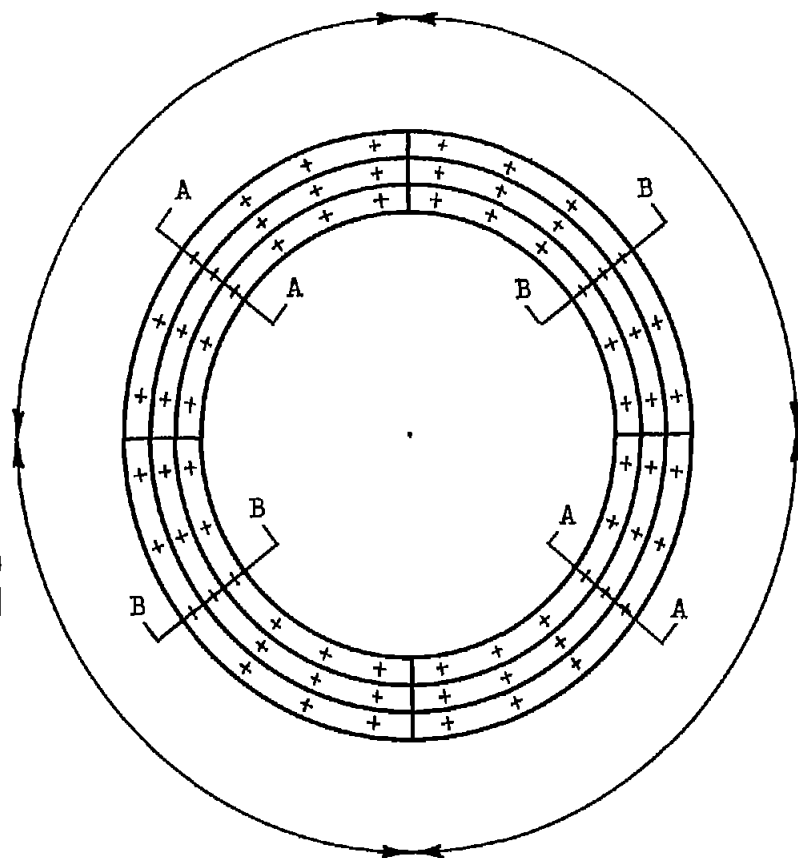
Section A-A



Injector D

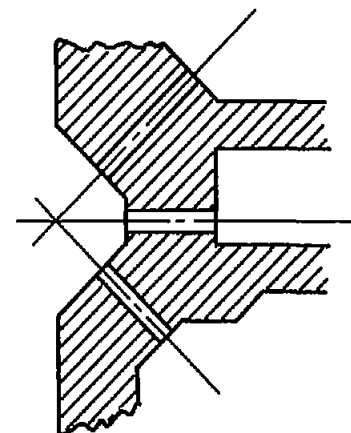
CD-4971

Figure 3. - Continued. Injectors.

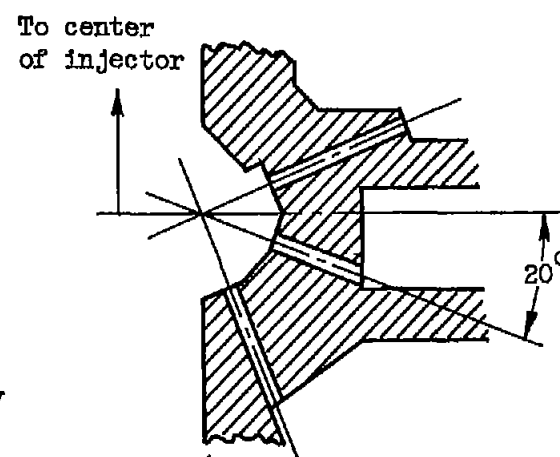


Injector E

CD-4972



Section A-A



Section B-B

Figure 3. - Concluded. Injectors.

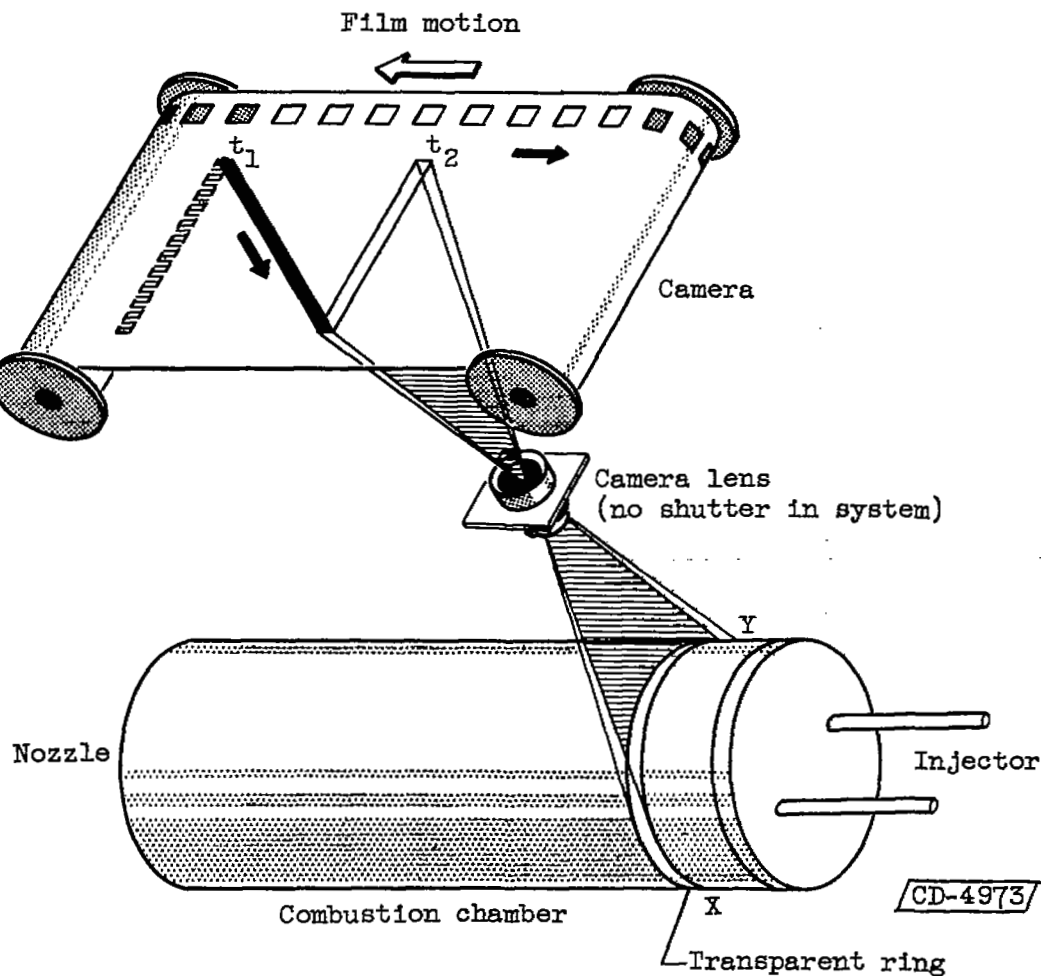


Figure 4. - Optics for moving-film streak photography. Image of window slit is represented on film at two different times t_1 and t_2 . If, during uniform velocity of film, a bright line moves linearly within the combustion chamber from **X** to **Y**, the solid line will be traced on the film.

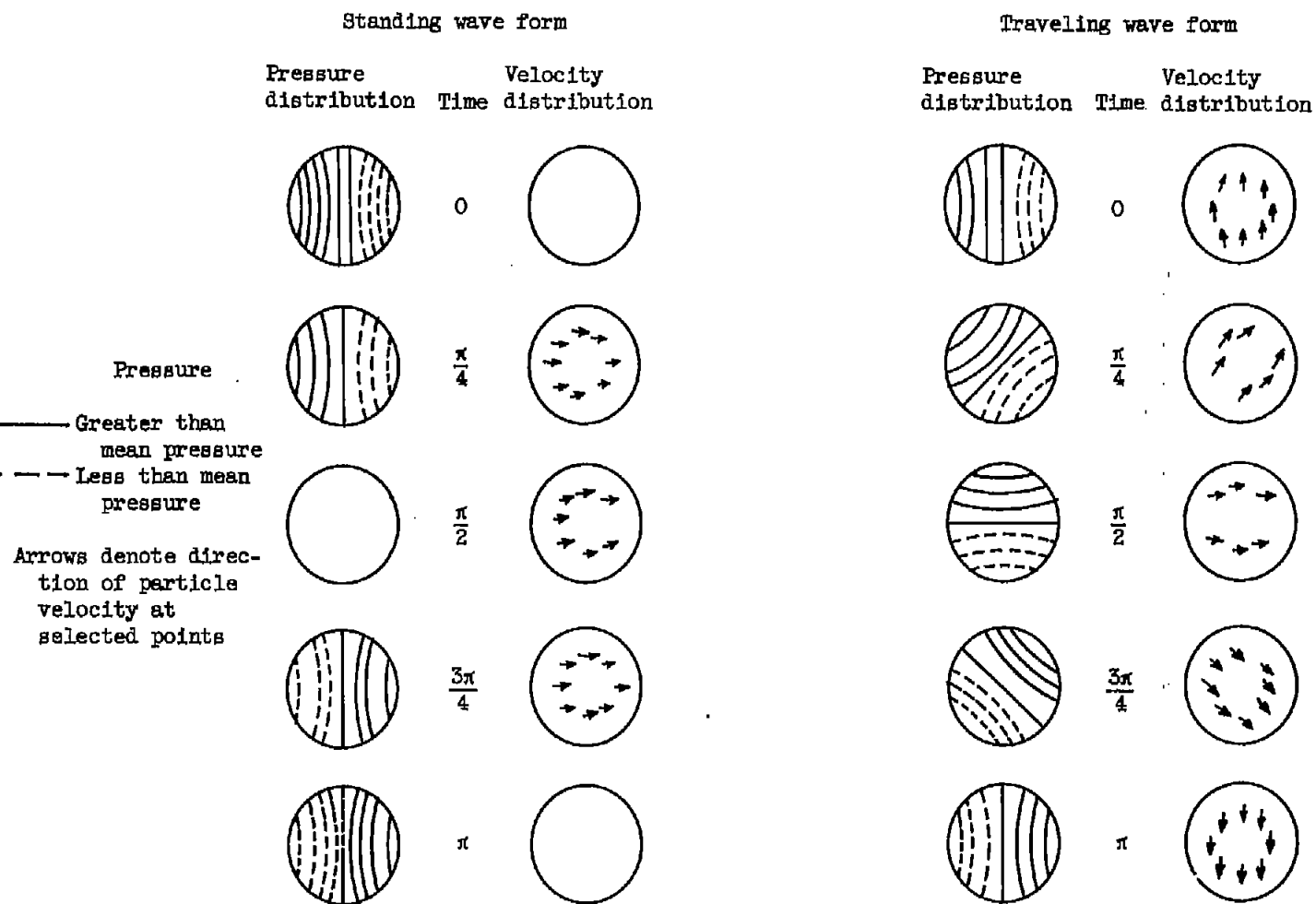
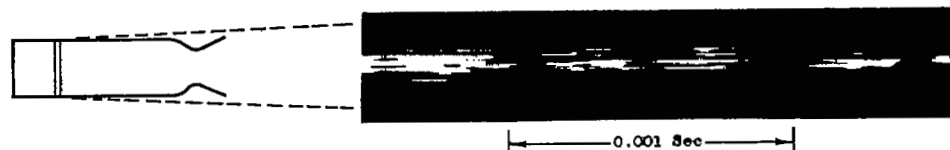


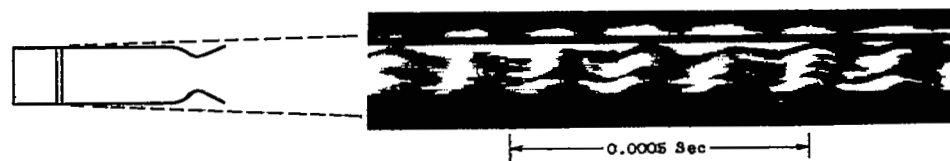
Figure 5. - Various forms of fundamental tangential mode of oscillation (reproduced from ref. 6).



(a) Smooth combustion.



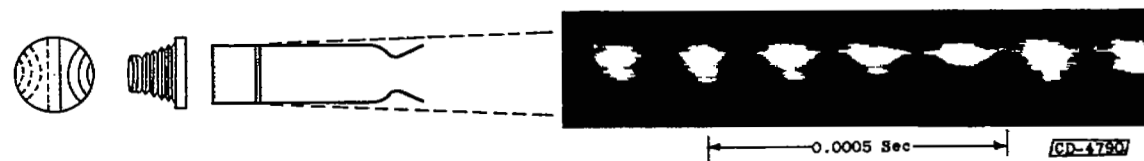
(b) Longitudinal wave.



(c) Traveling wave form of tangential mode.

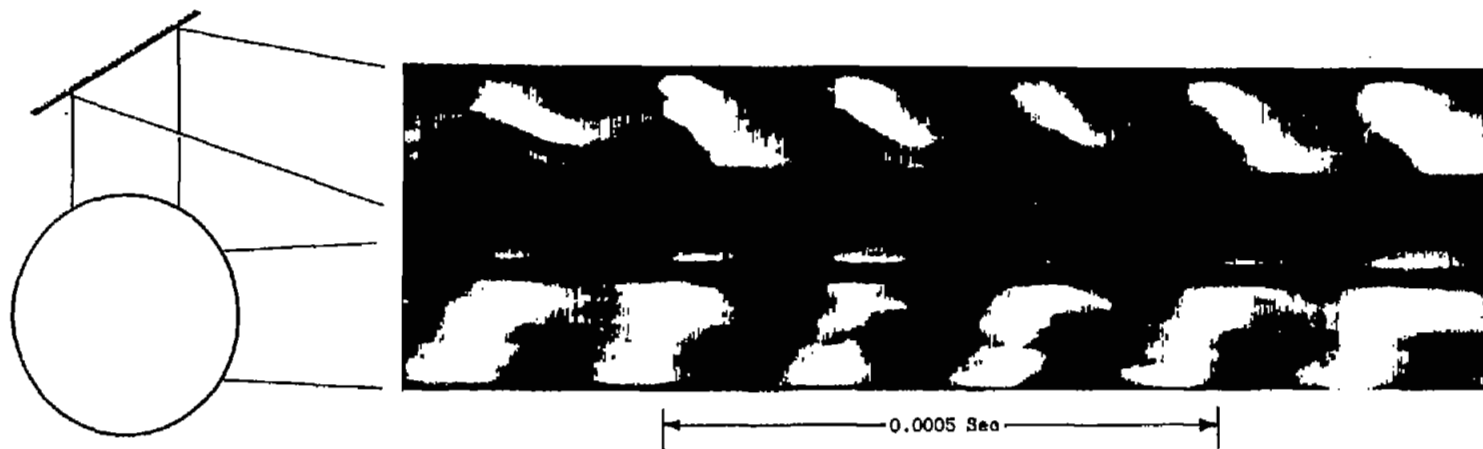


(d) Standing wave form of tangential mode viewed at anti-node point (zero pressure variation).



(e) Standing wave form of tangential mode viewed at node point (maximum pressure variation).

Figure 6. - Streak photographs of various oscillations in 1000-pound-thrust rocket engine using liquid oxygen and n-heptane as propellants.



(f) Traveling wave form of tangential mode; chamber viewed from two different angles.



(g) Standing wave form of tangential mode; chamber viewed from two different angles; camera aligned with nodes.

Figure 8. - Concluded. Streak photographs of various oscillations in 1000-pound-thrust rocket engine using liquid oxygen and n-heptane as propellants.

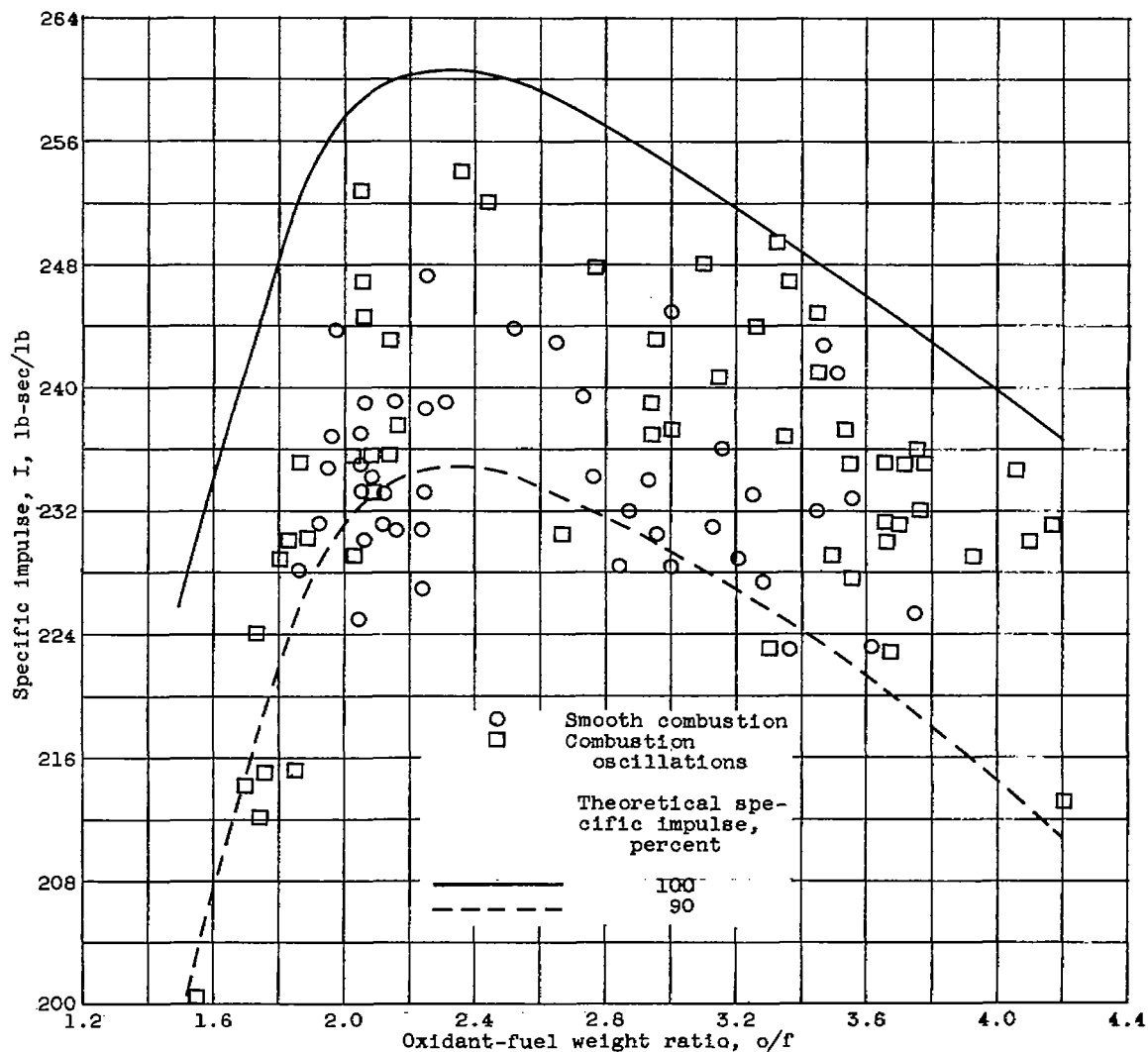


Figure 7. - Engine performance as a function of oxidant-fuel weight ratio (injector A). Combustion-chamber lengths, 8 to 32 inches; with and without fins; propellants, liquid oxygen and n-heptane.

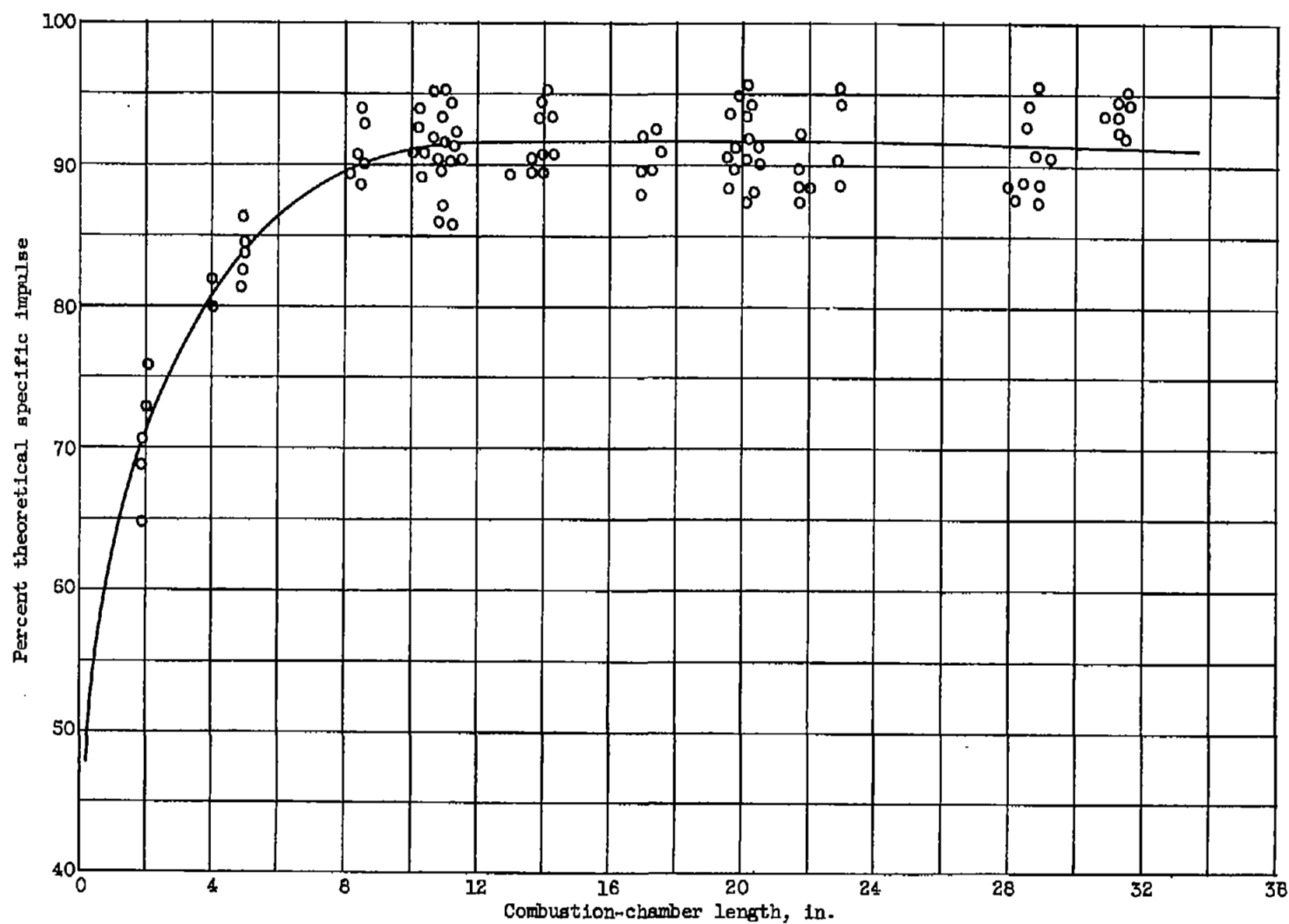


Figure 8. - Engine performance as a function of chamber length (injector A). Screaming and nonscreaming runs; with and without fins; propellants, liquid oxygen and n-heptane.

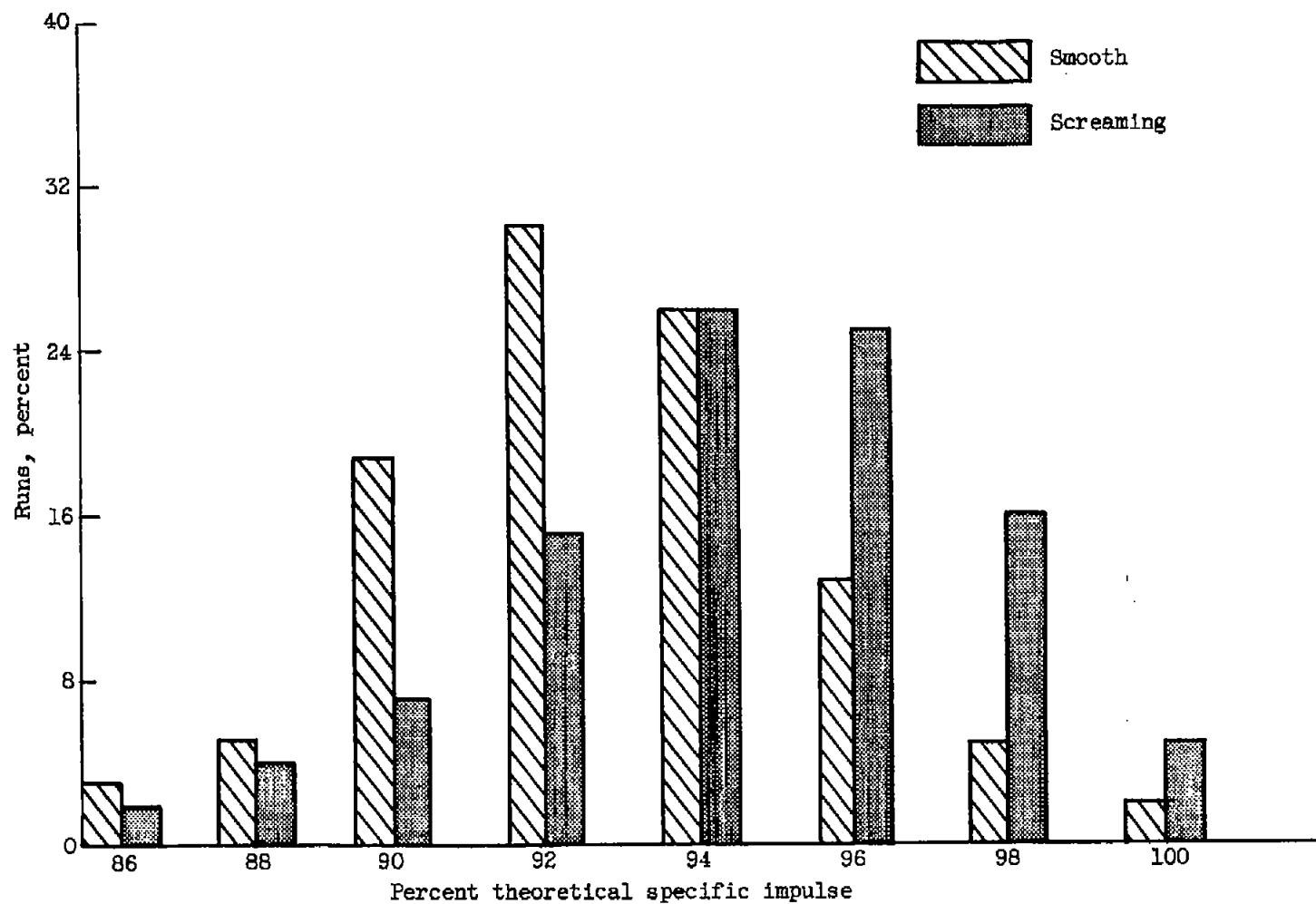
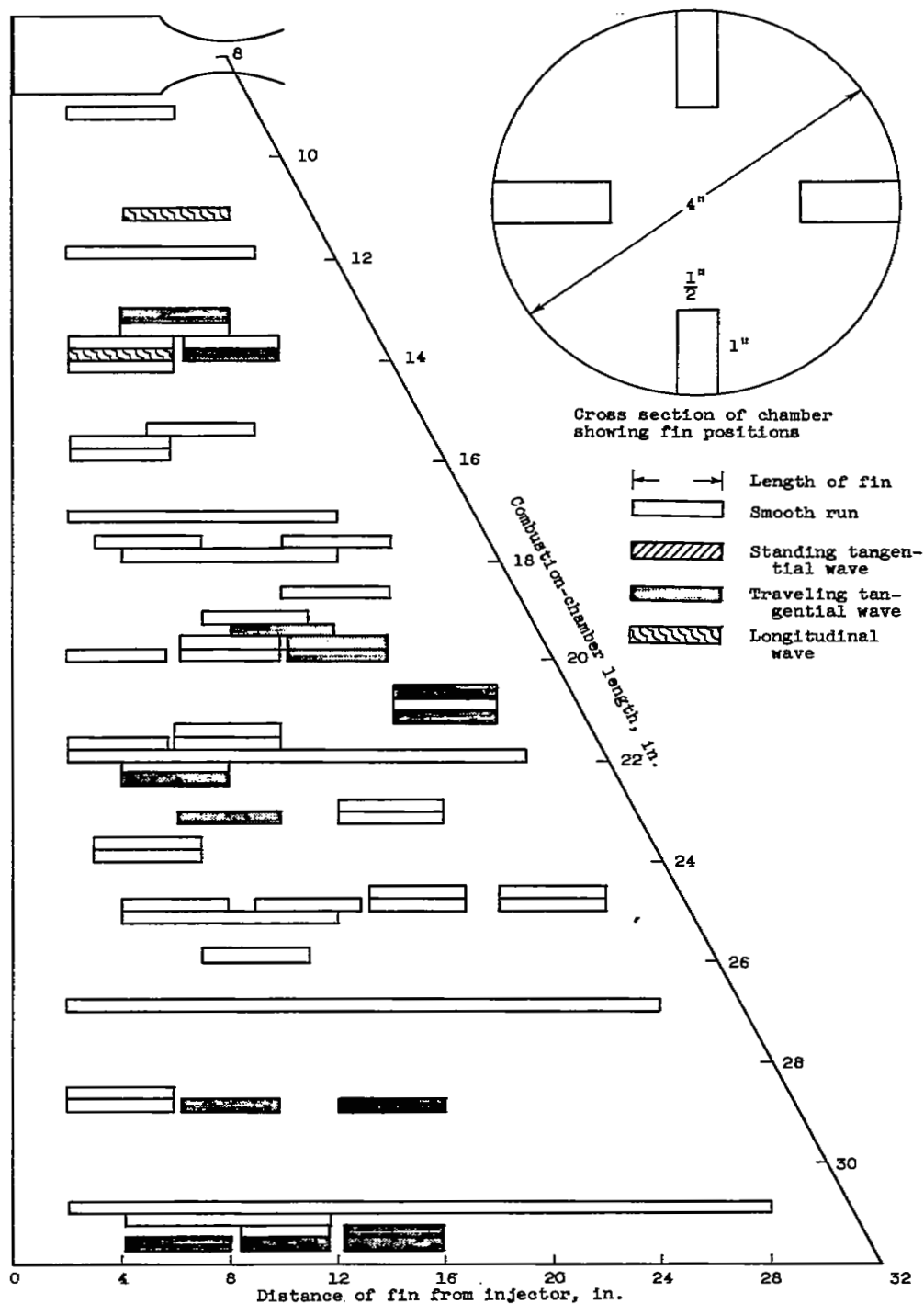
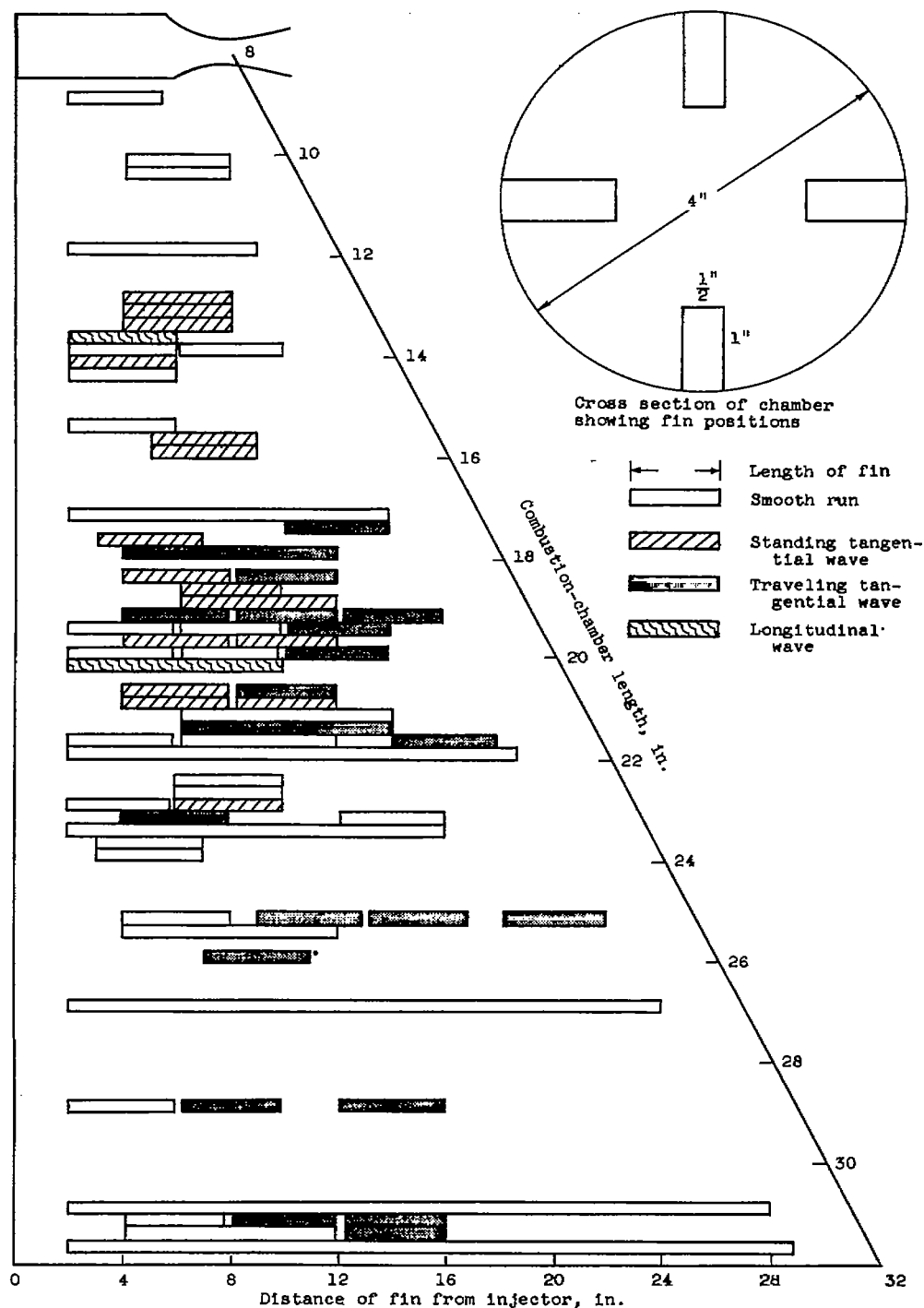


Figure 9. - Engine performance with smooth and screaming combustion for combustion-chamber lengths of 10 to 32 inches (injector A).



(a) Oxidant-fuel weight ratio, 1.5 to 2.5.

Figure 10 - Occurrence of screaming with various fin positions and engine lengths with 1000-pound-thrust rocket engine using liquid oxygen and n-heptane as propellants (injector A).



(b) Oxidant-fuel weight ratio, 2.5 to 4.0.

Figure 10. - Concluded. Occurrence of screaming with various fin positions and engine lengths with 1000-pound-thrust rocket engine using liquid oxygen and n-heptane as propellants (injector A).

CONFIDENTIAL

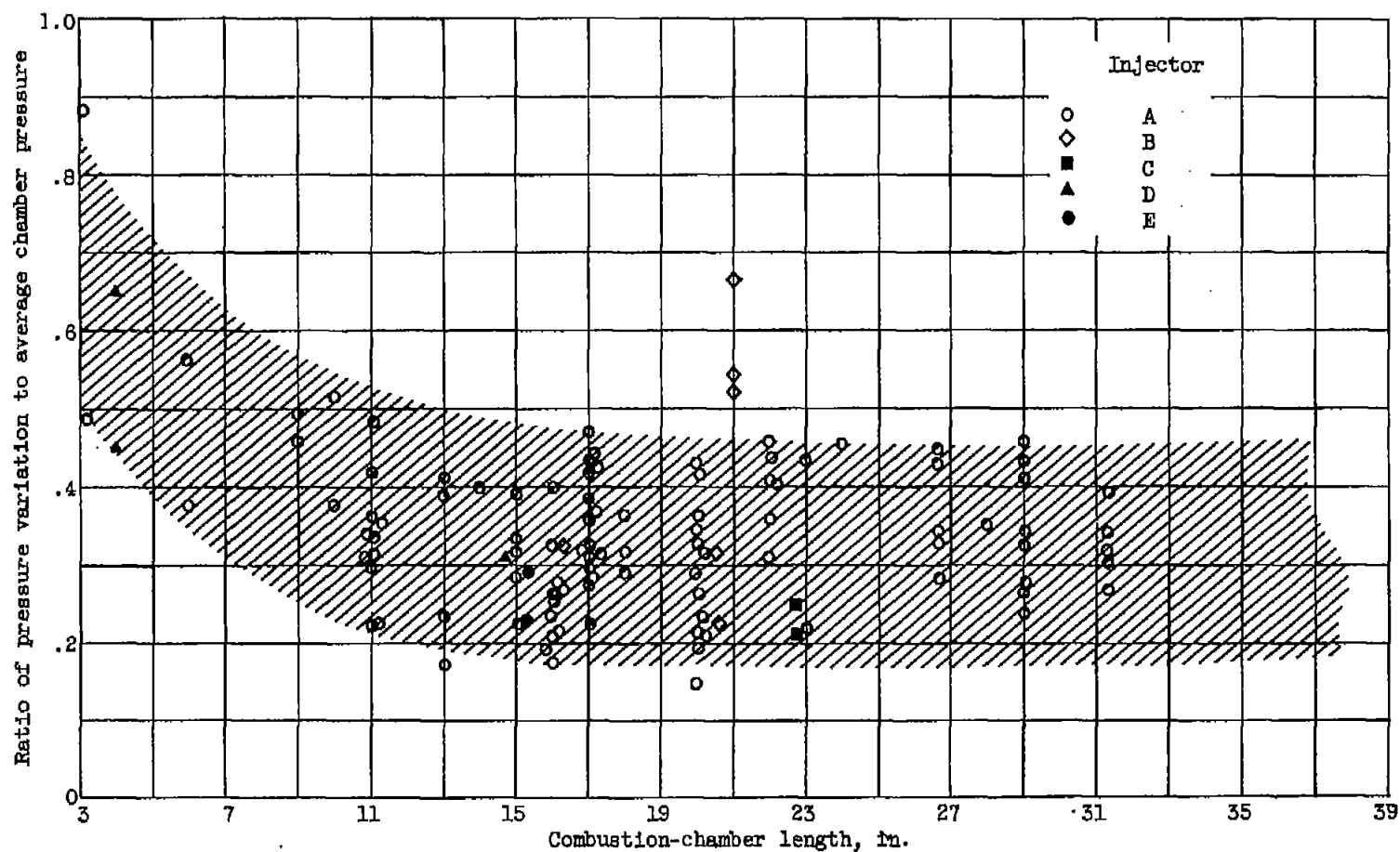


Figure 11. - Variation of amplitude of oscillating-wave pressure with combustion-chamber length for various injectors.

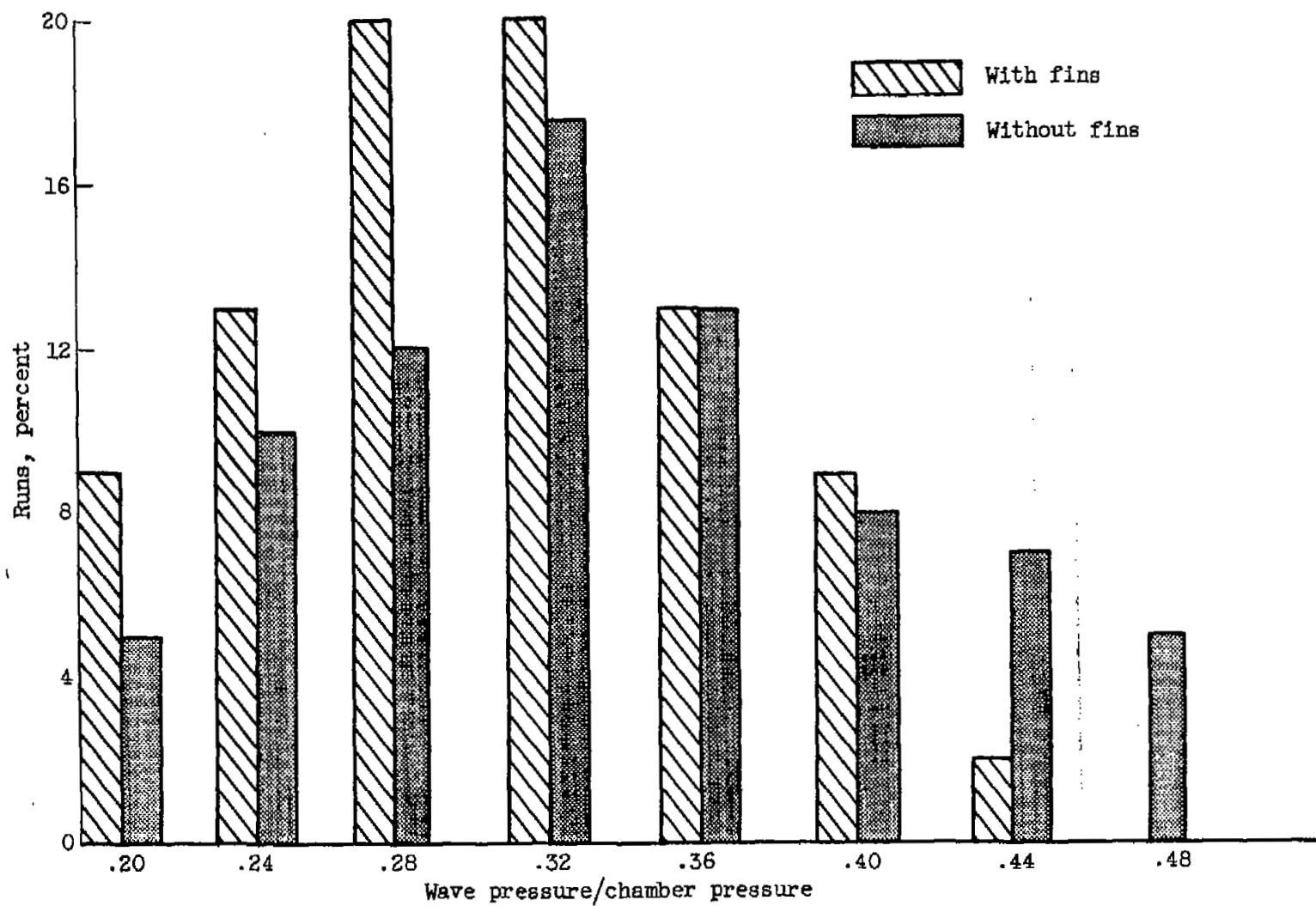
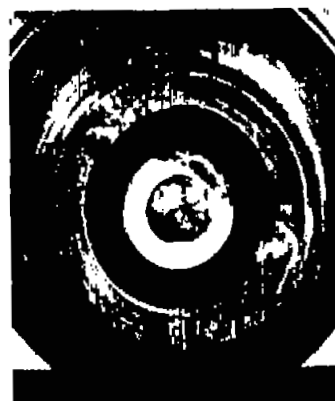


Figure 12. - Amplitude of oscillating wave pressure (injector A). Chamber length, 10 to 32 inches.



(a) Longitudinal oscillations.



(b) Traveling wave form of tangential oscillation.



Standing wave form of tangential oscillation

C-41410

(c) Spark plug located at node point
(maximum pressure variation).

(d) Spark plug located at anti-node point
(zero pressure variation).

Figure 13. - Burning of spark plug during screaming operation of rocket engine
(0.75-sec run) with various oscillations and spark plug locations.

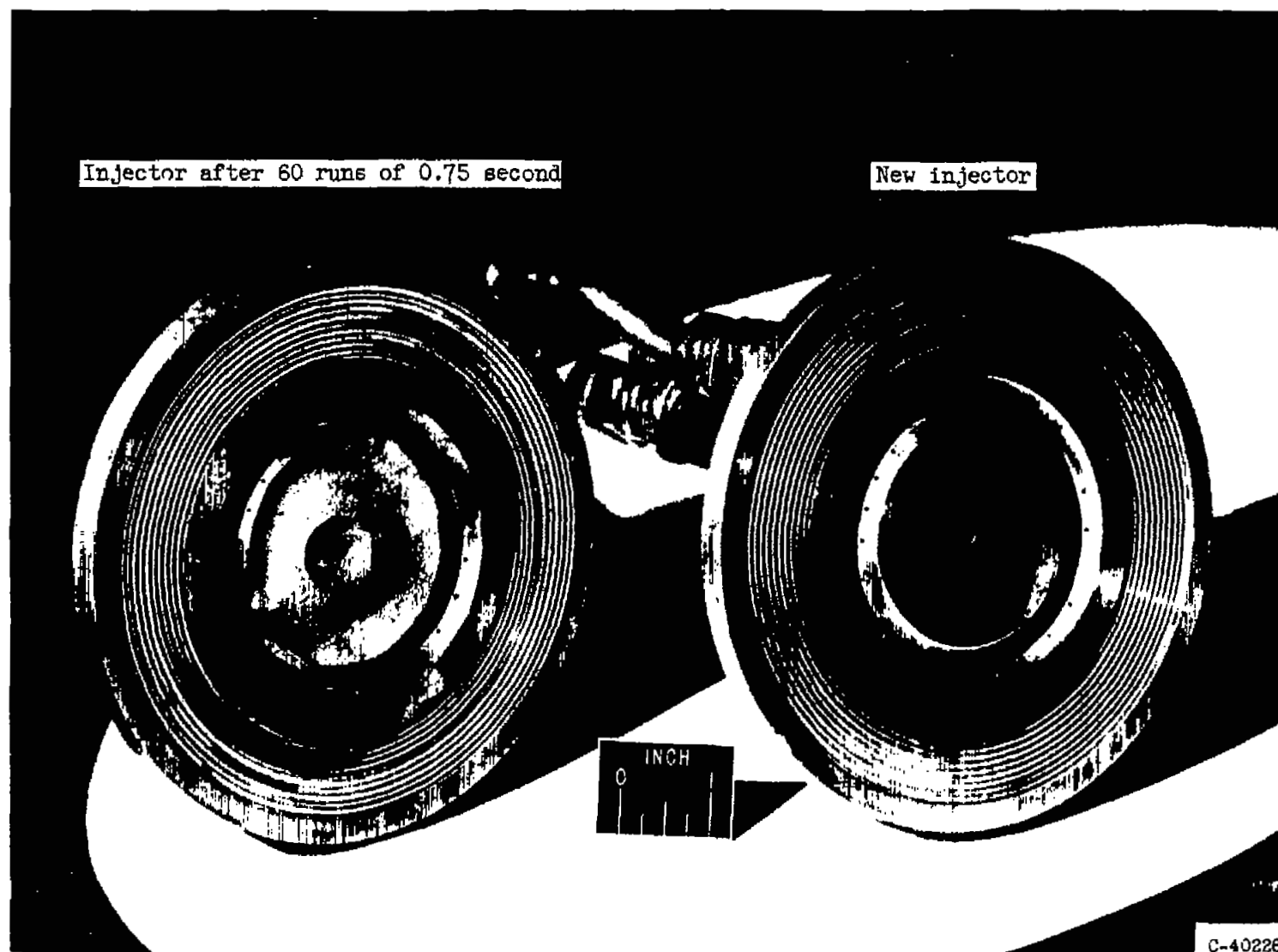
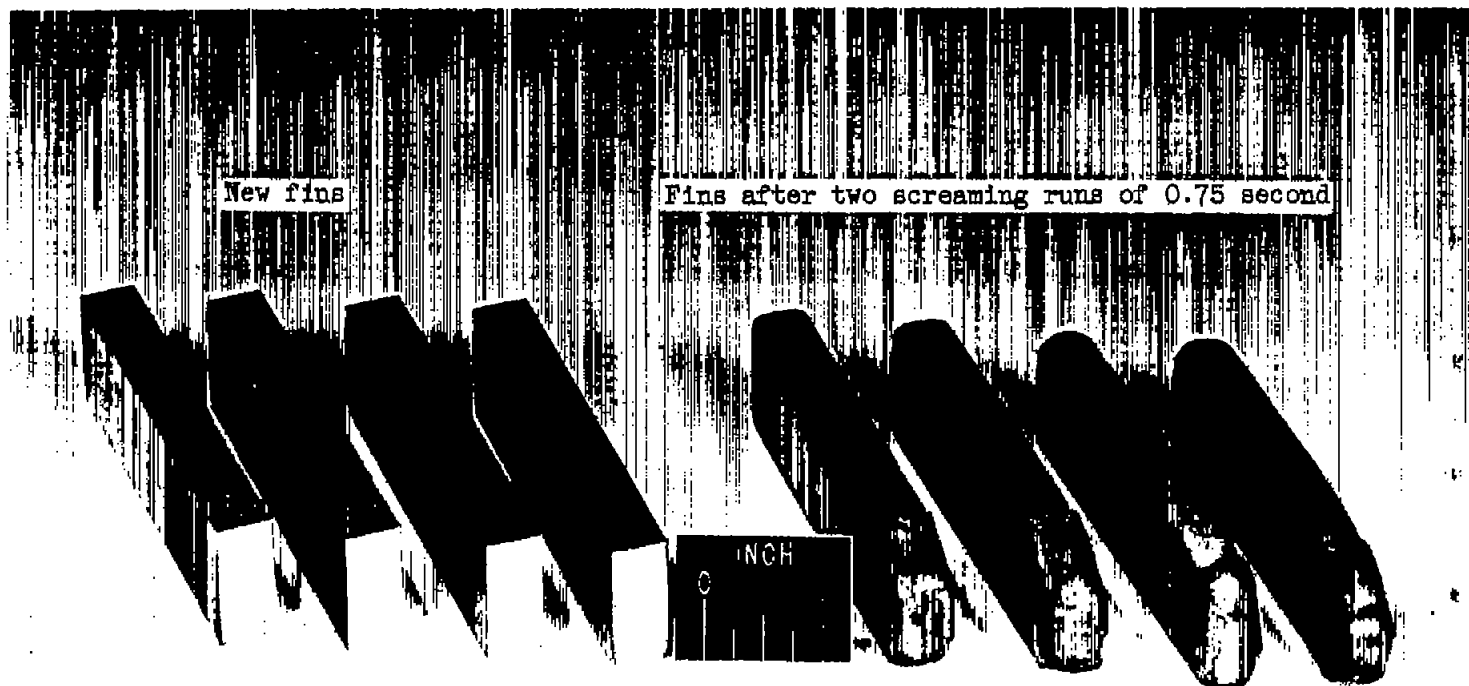


Figure 14. - Injector face illustrating burning obtained during runs.



C-40227

Figure 15. - Burning of fins caused by screaming operation of rocket engine.

NASA Technical Library



3 1176 01435 8361